Thermodynamic Properties of Niobium Oxides

K. T. Jacob,* Chander Shekhar, and M. Vinay

Department of Materials Engineering, Indian Institute of Science, Bangalore 560012, India

Yoshio Waseda

Institute of Multidisciplinary Research for Advanced Materials, Tohoku University, Sendai 980-8577, Japan

Thermodynamic properties of three oxides of niobium have been measured using solid state electrochemical cells incorporating yttria-doped thoria (YDT) as the electrolyte in the temperature range $T = (1000$ to $1300)$ K. The standard Gibbs energies of formation of NbO, NbO_2, and $NbO_{2.422}$ from the elements can be expressed as:

$$\triangle_f G^o_{NbO} \pm 547/\mathrm{J \cdot mol^{-1}} = -414\,986 + 86.861(T/\mathrm{K})$$

$$\triangle_f G^o_{NbO_2} \pm 548/\mathrm{J \cdot mol^{-1}} = -779\,864 + 164.438(T/\mathrm{K})$$

$$\triangle_f G^o_{NbO_{2.422}} \pm 775/\mathrm{J \cdot mol^{-1}} = -911\,045 + 197.932(T/\mathrm{K})$$

The results are discussed in comparison with thermodynamic data reported in the literature. The new results refine data for NbO and NbO_2 presented in standard data compilations. There are no data in thermodynamic compilations for $NbO_{2.422}$ ($Nb_{12}O_{29}$). In the absence of the heat capacity and enthalpy of formation measurements, only the Gibbs energy of formation of $NbO_{2.422}$ can be assessed. The free energy of formation of stoichiometric Nb_2O_5 is evaluated on the basis of measurements on $NbO_{2.422}$ and information available in the literature on phase boundary compositions and isothermal variation of nonstoichiometric parameter with oxygen potential for Nb_2O_{5-x}. The results suggest a minor revision of data for Nb_2O_5. A minimum in the Gibbs energy of mixing for the system Nb−O occurs in the nonstoichiometric domain of Nb_2O_{5-x} with $x = 0.036$.

Introduction

Refractory metal niobium (Nb) is a promising structural material for the first wall of nuclear fusion reactors.[1] However, it has great affinity for oxygen, nitrogen, and carbon present in the plasma and coolants such as liquid alkali metals and helium gas. As a potential material for the first wall, niobium is known to react most readily with oxygen. Consequently, it is useful to have accurate thermodynamic data on niobium oxides, NbO, NbO_2, Nb_2O_5, and other intermediate phases such as $Nb_{12}O_{29}$. Apart from this, oxides of niobium have other advanced applications. Niobium monoxide (NbO) is used as a gate electrode in n-channel metal-oxide-semiconductor field effect transistors (NMOS-FET)[2] and a NbO/NbO_2 junction can be used in high-speed high-current switching devices.[3] The threshold switching of NbO_2 using single-crystal or polycrystalline samples[4,5] can be used in ultrafast electromagnetic pulse protection devices. Using amorphous NbO_2 thin films,[6] monostable switching devices have also been prepared. Nb_2O_5 exhibits a high dielectric constant[7] and electrochromism.[8−10] Nb_2O_5 is an excellent catalyst for the polymerization of propylene,[11] dehydration of 2-butanol,[11] and butene isomerization.[11,12] Nb_2O_5 deposited on Pt foil can function as a thin film capacitor.[13]

The phase diagram of the Nb−O system compiled by Massalski et al.[14] shows NbO, NbO_2, and Nb_2O_5 as the only stable oxide phases. More recent research on phase equilibria in the system Nb−O[15−19] has revealed the existence of several other oxide phases. Kimura[15] studied the NbO_2−Nb_2O_5 system at $T = (1573$ and $1673)$ K and reported that five additional phases, $Nb_{12}O_{29}$, $Nb_{22}O_{54}$, $Nb_{47}O_{116}$, $Nb_{25}O_{62}$, and $Nb_{53}O_{132}$, were stable over different temperature ranges. The existence of two nonstoichiometric compounds "$NbO_{2.42}$" and "$NbO_{2.47}$" in the temperature range $T = (1273$ to $1373)$ K had been reported by Marucco.[16] Naito et al.[17] measured electrical conductivities of the different phases between NbO_2 and Nb_2O_5 as a function of oxygen partial pressure in the temperature range $T = (1283$ to $1573)$ K. On the basis of the breaks in the conductivity plots, regions of existence of the intermediate phases were deduced. A phase diagram for the Nb−O system between $1.99 \leq$ O/Nb ≤ 2.50 and $T = (1173$ to $1673)$ K was presented. Naito and Matsui[18] reviewed the phase relations, defect structure, and partial molar properties of oxygen in the Nb−O system. Matsui

* Corresponding author. Tel.: +91-80-22932494. Fax: +91-80-23600472. E-mail address: katob@materials.iisc.ernet.in (K. T. Jacob).

10.1021/je1004609
Published on Web 08/20/2010

and Naito[19] studied the thermodynamic properties of niobium oxides with a O/Nb ratio between 2.47 and 2.50 using a galvanic cell in the temperature range T = (1084 to 1325) K and confirmed the phase diagram for the system Nb−O presented by Naito et al.[17]

Of all the reported phases, NbO, NbO_2, $Nb_{12}O_{29}$ ($NbO_{2.417}$), and nonstoichiometric Nb_2O_{5-x} are stable at T = 1223 K.[17−19] Thermodynamic properties of NbO, NbO_2, and Nb_2O_5 have been measured by various authors[20−30] and are compiled by Schick,[31] NIST-JANAF tables,[32] and Pankratz and Mrazek,[33] assuming the presence of only three stable oxide phases, NbO, NbO_2, and Nb_2O_{5-x}. Although there are three measurements[16,20,26] of oxygen potential involving $Nb_{12}O_{29}$, comprehensive thermodynamic data for this compound are not found in thermodynamic compilations. Available thermodynamic data are not fully consistent with the phase diagram.[17] Therefore, new measurements were conducted to resolve conflicts and refine data.

The standard Gibbs energy of formation of NbO has been measured by different authors[20−25] employing solid state electrochemical cells based on doped ThO_2 as the electrolyte. Used as the reference electrode by Worrell[20] and Hiraoka et al.[21] was a mixture of (NbO + NbO_2) and (Cr + Cr_2O_3), respectively, having oxygen chemical potentials moderately higher than that of the measuring electrode of (Nb + NbO). Ignatowicz and Davies,[22] Drobyshev and Rezukhina,[23] Lavrentév et al.,[24] and Steele and Alcock[25] used a mixture of (Fe + "FeO") as the reference electrode having an oxygen chemical potential significantly higher than that of the measuring electrode. The Gibbs energies of formation of NbO reported by Ignatowicz and Davies,[22] Drobyshev and Rezukhina,[23] and Steele and Alcock[25] are significantly more positive than values reported by Worrell[20] and Hiraoka et al.[21] The oxygen potential associated with the mixture of (Nb + NbO) is close to the lower oxygen potential boundary for predominant ionic conduction (ionic transport number > 0.99) in doped-ThO_2 electrolytes. The ionic conduction domain extends from an oxygen fugacity of 10^{-6} to 10^{-26} at T = 1273 K. Close to the boundary of ionic conduction, polarization of electrodes caused by trace electronic conductivity and consequent oxygen flux from the electrode with higher oxygen fugacity to one with lower oxygen fugacity becomes a cause for concern. The larger the oxygen fugacity difference between the reference and the measuring electrodes, the larger the error caused by electrode polarization is. In this study, (Mn + MnO), having an oxygen fugacity between that of (NbO + NbO_2) and (Cr + Cr_2O_3), was selected as the reference electrode. This choice results in a relatively small electromotive force (emf) and provides additional validation of thermodynamic data. Accurate values for the Gibbs energy of formation of MnO (± 250 J·mol^{-1}) are available from recent measurements and assessment.

The Gibbs energy of formation of NbO_2 has been measured by Hiraoka et al.[21] and Marucco et al.[26] using a solid state electrochemical cell based on doped ThO_2 as the electrolyte employing a mixture of (Cr + Cr_2O_3) as the reference electrode in the temperature ranges T = (1117 to 1361) K and T = (1173, 1273, and 1323) K, respectively. Steele and Alcock[25] measured the Gibbs energy of formation of NbO_2 using doped ThO_2 as the electrolyte and (Fe + "FeO") as the reference electrode at T = 1273 K. Worrell[27] measured the CO equilibrium partial pressure in the temperature range T = (1050 to 1200) K for the reduction of Nb_2O_5 to NbO_2 by solid carbon.

Recently, Wenger and Keesom[28] measured the low temperature heat capacity of single crystal NbO_2 in the temperature range T = (2.5 to 30) K using the standard heat pulse technique. Seta and Naito[34] measured the heat capacity of NbO_2 in the temperature range T = (400 to 1170) K using direct heating pulse calorimetry and reported an anomaly in the heat capacity measurement corresponding to a phase transition at T = 1080 K. Since more extensive data on low and high temperature heat capacity of NbO_2 are now available, the re-evaluation of the thermodynamic properties of NbO_2 is in order. For internal consistency, it is useful to update the thermodynamic properties of NbO as well.

NbO has a cubic structure with lattice parameter a = 0.42101 nm and space group $Pm3m$.[35] NbO_2 occurs in two different forms.[34,36] A phase transition occurs from a low-temperature distorted rutile structure ($I4_1/a$, a = 1.3702 nm, c = 0.5985 nm) to a high-temperature rutile ($P4_2/mnm$, a = 0.48463 nm, c = 0.30315 nm) having a body centered tetragonal cell at T_{tr} = 1080 K. The low-temperature structure is a distorted rutile type with NbO_6 octahedra joined by edges and corners. Nb−Nb distances along the c-axis vary alternatively as short and long. The high temperature rutile form adopts a four long, two short Nb−O bond pattern.[36] $Nb_{12}O_{29}$ crystallizes as orthorhombic[37] ($Cmcm$, a = 0.38320 nm, b = 2.07400 nm, c = 2.88901 nm) and monoclinic[38] ($A2/a$, a = 3.132 nm, b = 0.3832 nm, c = 2.072 nm; β = 112.93°) forms. A recent study[39] indicates that the low temperature monoclinic phase transforms to the orthorhombic phase over the temperature range T = (1473 to 1673) K. Although, Nb_2O_5 exists in several modifications; the α (or H) form is considered to be the thermodynamically stable modification.[40] α-Nb_2O_5 has a monoclinic structure (space group $P2$) with lattice parameters a = 2.115 nm, b = 0.3831 nm, and c = 1.937 nm.[41]

The homogeneity range for NbO, determined from the samples quenched from the melting point to room temperature is 0.98 ≤ O/Nb ≤ 1.02.[42] According to the phase diagram for the Nb−O system proposed by Naito et al.,[17] the homogeneity ranges for NbO_2 and $Nb_{12}O_{29}$ at T = 1223 K are 1.9995 ≤ O/Nb ≤ 2.0023 and 2.4230 ≤ O/Nb ≤ 2.4330, respectively. The homogeneity range of the nonstoichiometric Nb_2O_{5-x} phase has been determined by X-ray diffractometry,[43,44] chemical analysis,[44] thermogravimetry,[16,45,46] electrical conductivity,[16] and electrochemical measurement.[47] Early studies by Brauer[43] and Blumenthal et al.[47] indicated a wide nonstoichiometric region ranging from $NbO_{2.5}$ to approximately $NbO_{2.4}$ with the oxygen deficient component in equilibrium with NbO_2. Subsequent studies reported a relatively narrower homogeneity range for Nb_2O_{5-x} and other intermediate oxide phases between NbO_2 and Nb_2O_{5-x}: Marucco[16,46] ((2.485 to 2.491) ≤ O/Nb ≤ 2.5; 1273 ≤ T ≤ 1373 K), Naito et al.[17] (2.484 ≤ O/Nb ≤ 2.5; T = 1333 K), Schafer et al.[44] (2.489 ≤ O/Nb ≤ 2.5; T = 1573 K), and Kofstad and Anderson[45] (2.48 ≤ O/Nb ≤ 2.50; T = 1200 K).

Experimental Section

Materials. Powders of Nb, Mn, Nb_2O_5, and Mn_2O_3, each of mass fraction purity higher than 0.9999, were used to prepare the electrodes. Puratronic grade Nb and Nb_2O_5 were obtained from Alfa Aesar. Nb_2O_5 powder was heated at T = 1273 K for 36 ks in dry air to ensure the formation of α-Nb_2O_5. Mn_2O_3 was heated in air at T = 1073 K for 30 ks to remove moisture and other volatiles. NbO was produced by sintering a mixture of α-Nb_2O_5 and Nb in the required ratio under vacuum. NbO was then mixed in the appropriate ratio with α-Nb_2O_5 and reacted at T = 1273 K for ~173 ks to give NbO_2 and $NbO_{2.417}$ ($Nb_{12}O_{29}$). However, the sample of stoichiometric composition $Nb_{12}O_{29}$ was found to contain traces of NbO_2 when examined

under scanning and transmission electron microscopes. A single phase product was obtained at a slightly higher oxygen concentration $NbO_{2.422}$, in agreement with Naito et al.[17] Formation of the required compounds was confirmed by X-ray diffraction (XRD). The composition of the samples was confirmed by gravimetric oxidation. The particle size of the powders used was in the range of (5 to 20) μm. Yttria-doped thoria (YDT), used as the solid electrolyte in the electrochemical cell, was prepared using the method reported elsewhere.[48] The measuring electrode was prepared by mixing Nb and NbO in the molar ratio 1.25:1, compacting the mixture into pellets using a hardened steel die at $p = 100$ MPa, and sintering at $T = 1373$ K in a stream of prepurified argon gas for ~30 ks. Bright green MnO powder was prepared by reducing Mn_2O_3 contained in a platinum boat in a stream of dry hydrogen at $T = 1300$ K for ~15 ks. Formation of MnO having the rock salt structure with the lattice parameter $a = 0.4446$ nm was confirmed by XRD. The reference electrode (Mn + MnO) of cell I was prepared by compacting a mixture of Mn and MnO in the molar ratio 1:1.25 and sintering under conditions identical to that used for the measuring electrode of cell I. Mixtures of (NbO and NbO_2) were taken in the ratio 1:1.25 to form the electrode in cell II and in the ratio 1.25:1 in cell III. The mixture of (NbO_2 and $NbO_{2.422}$) was compacted in the molar ratio 1:1.25 to form the electrode in cell III. The electrodes were sintered under conditions similar to that employed for the measuring electrode of cell I. In each electrode an excess of the phase that was consumed by the electrochemical flux of oxygen through the solid electrolyte was used. Argon gas of mass fraction purity higher than 0.99999 was used in this study and was dried by passing through columns of anhydrous silica gel, magnesium perchlorate, and diphosphorus pentoxide and deoxidized by passage through a titanium sponge at $T = 1123$ K prior to use.

Apparatus. The apparatus used in this study was similar to the one described elsewhere.[49] Reference and working electrodes were spring loaded against two polished surfaces of a dense YDT electrolyte pellet by a rig consisting of alumina rings and slabs. The assembly was suspended inside an alumina tube flushed with prepurified Ar gas. The space around the measuring electrode was isolated by a second alumina tube spring loaded against the YDT electrolyte pellet. The alumina tube surrounding the measuring electrode was also flushed with a separate stream of prepurified Ar gas. With this arrangement the gas atmosphere around the two electrodes was physically separated, thus preventing transport of oxygen and manganese between the electrodes via the gas phase. For each cell the reversible emf was measured as a function of temperature at regular intervals in the range $T =$ (1000 to 1300) K. The cells were placed in the constant temperature (± 1 K) zone of a vertical resistance-heated furnace.

Because of the very low oxygen partial pressure over the electrodes, it is necessary to remove oxygen-bearing species from the gas phase surrounding the electrodes. Titanium internal getters were placed in the path of incoming Ar streams at a location approximately 70 mm from the cell where the temperature was ~250 K below that of the cell. The internal getters removed residual oxygen in the Ar and oxygen from H_2O, CO, and CO_2 gas species that desorbed gradually from the alumina tubes and supports at high temperature. The position of the internal getters was adjusted such that the oxygen partial pressure in Ar gas was of the same order as that prevailing over the electrode. The electrical contact to the electrodes was made by insulated platinum leads. Insulation was provided by an alumina thermal spray coating. The temperature of the cell was measured by a Pt/Pt-13%Rh thermocouple placed adjacent to the cell within 2 mm. The thermocouple was checked against the melting point of Au. The electrodes were examined by XRD before and after each experiment. No change was detected in the phase composition of the electrodes during high temperature measurements.

Procedure. The solid state electrochemical cells used in this study can be represented as:

$$\text{Pt, Nb + NbO//}(Y_2O_3)ThO_2\text{//Mn + MnO, Pt} \quad \text{(Cell I)}$$

$$\text{Pt, Nb + NbO//}(Y_2O_3)ThO_2\text{//NbO + }NbO_2\text{, Pt} \quad \text{(Cell II)}$$

$$\text{Pt, NbO + }NbO_2\text{//}(Y_2O_3)ThO_2\text{//}NbO_2\text{ + }NbO_{2.422}\text{, Pt} \quad \text{(Cell III)}$$

The cells are written such that the right-hand electrodes are positive. After assembling the cell, the outer alumina tube enclosing the cell was evacuated to a pressure of 10 Pa and then refilled with prepurified Ar gas. This procedure was repeated after heating the cell to $T = 850$ K to remove most of the oxygen-bearing gas species that were initially adsorbed on the ceramic tubes. The molecules that desorbed at the higher temperatures were captured by the internal getters. After the attainment of constant temperature, the cell registered a constant emf in (1.2 to 3.8) ks depending on temperature; longer periods were required at lower temperatures. The reversible emf of the cell I was measured in the temperature range from $T =$ (1000 to 1300) K at intervals of 25 K using a high impedance (> 10^{12} Ω) digital voltmeter. Below $T = 1000$ K, there was a small drift in emf with time and reversibility, and reproducibility was poor. The vapor pressure of Mn set the upper limit of temperature for cell operation.

The reversibility of the cells was checked by passing small direct current (~10 μA) through the cell for ~0.3 ks in the either direction using an external circuit. The current caused polarization of the electrode and the cell voltage was displaced from the equilibrium value. However, the cell voltage was found to approach the steady value before titration after (0.8 to 2) ks depending on the operating temperature of the cell. Since the cell voltage returned to the same value after successive displacement in the opposite directions, reversibility was ascertained. The cell emf was also found to be independent of the flow rate of inert gas over the electrode and to be reproducible on temperature cycling.

Results

Plotted in Figure 1 are variations of reversible emf of the solid state electrochemical cells as a function of temperature in the range $T =$ (1000 to 1300) K using a different emf scale for each cell. Within the experimental error, the emf of each cell is a linear function of temperature. The least-squares regression analysis gives:

$$E_1 \pm 1.153/\text{mV} = 140.6 - 0.0596(T/\text{K}) \quad (1)$$

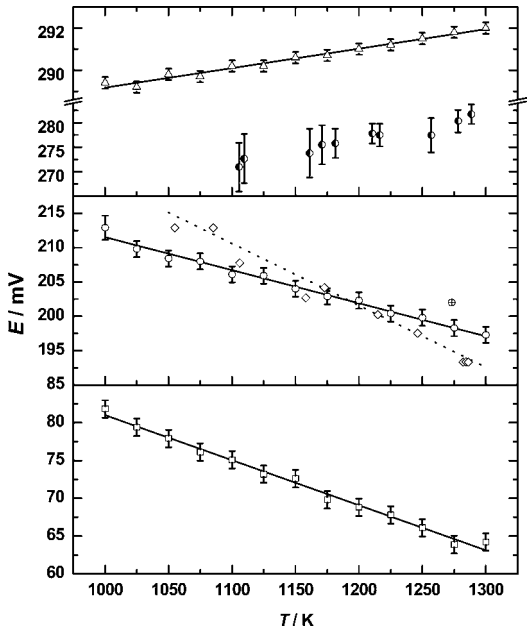

Figure 1. Temperature dependence of reversible emf of the solid state electrochemical cells studied. □, cell I (this study); ○, cell II (this study); ◇, cell II (Worrell[20]); ⊕, cell II (Steele and Alcock[25]); △, cell III (this study); ◐, cell III (Worrell[20]); —, least-squares regression analysis of the emf of each cell measured in this study; ····, equation for the emf of cell II reported by Worrell.[20]

$$E_2 \pm 1.166/\text{mV} = 259.6 - 0.0481(T/\text{K}) \qquad (2)$$

$$E_3 \pm 0.269/\text{mV} = 279.95 + 0.00923(T/\text{K}) \qquad (3)$$

where the uncertainty limit corresponds to twice the standard error estimate. The phase transition of NbO_2 at $T = 1080$ K is not reflected in the emf variation with temperature of cells II and III, probably because the transition occurs close to the lower end of the temperature range of measurement at $T = 1000$ K. Because of the relatively small enthalpy change associated with phase transition and the uncertainty in the measurement of emf, the small change in slope expected below the transition temperature could not be identified with significant statistical confidence. The emf of each cell is related to the difference in the chemical potential of oxygen at the two electrodes by the Nernst equation; $\Delta\mu^{W}_{O_2} - \Delta\mu^{R}_{O_2} = -4FE$, where superscripts W and R denote the working and reference electrodes, respectively. For cell I, the oxygen potential for the reference electrode (Mn + MnO) is given by:[48]

$$\Delta\mu^{R}_{O_2} \pm 500/\text{J·mol}^{-1} = -775\,700 + 150.72(T/\text{K}) \qquad (4)$$

From the reversible emf of cell I, the oxygen potential at the working electrode and the standard Gibbs energy of formation of NbO, according to the reaction $Nb + 1/2O_2 \rightarrow NbO$, are obtained;

$$\Delta_f G^{o}_{NbO} \pm 547/\text{J·mol}^{-1} = \Delta\mu^{W}_{O_2}/2 = -414\,986 + 86.861(T/\text{K}) \qquad (5)$$

Similarly, from the reversible emf of cell II, the oxygen potential of the working electrode ($NbO + NbO_2$) defined by the reaction, $2NbO + O_2 \rightarrow 2NbO_2$, is obtained as:

$$\Delta\mu^{W}_{O_2}/\text{J·mol}^{-1} = -729\,756 + 155.154(T/\text{K}) \qquad (6)$$

Using the Gibbs energy of formation of NbO and the oxygen potential of the working electrode of cell II, the standard Gibbs energy of formation of NbO_2 from elements can be calculated as:

$$\Delta_f G^{o}_{NbO_2} \pm 548/\text{J·mol}^{-1} = -779\,864 + 164.438(T/\text{K}) \qquad (7)$$

From the reversible emf of cell III, the oxygen potential of the working electrode of cell III ($NbO_2 + NbO_{2.422}$) defined by the reaction, $(1000/211)NbO_2 + O_2 \rightarrow (1000/211)NbO_{2.422}$ is given by;

$$\Delta\mu^{W}_{O_2}/\text{J·mol}^{-1} = -621\,712 + 158.716(T/\text{K}) \qquad (8)$$

From the Gibbs energy of formation of NbO_2 and oxygen potential of the working electrode of cell III, the Gibbs energy of formation of $NbO_{2.422}$ is given by;

$$\Delta_f G^{o}_{NbO_{2.422}} \pm 775/\text{J·mol}^{-1} = -911\,045 + 197.932(T/\text{K}) \qquad (9)$$

The temperature-independent terms on the right-hand side of eqs 5, 7, and 9 represent the enthalpy of formation from the elements (ΔH^{o}_f/kJ·mol^{-1}) of NbO, NbO_2, and $NbO_{2.422}$ at a mean experimental temperature of $T = 1150$ K. The temperature-dependent terms in these equations are related to the corresponding entropy of formation (ΔS^{o}_f/J·mol^{-1}·K^{-1}) of NbO, NbO_2, and $NbO_{2.422}$ at the mean temperature. Thus, the second-law enthalpies of formation (ΔH^{o}_f/kJ·mol^{-1}) at $T = 1150$ K are −414.986 for NbO, −779.864 for NbO_2, and −911.045 for $NbO_{2.422}$, respectively. The corresponding entropies of formation (ΔS^{o}_f/J·mol^{-1}·K^{-1}) at the mean temperature are −86.861 for NbO, − 164.438 for NbO_2, and −197.932 for $NbO_{2.422}$. Because of the phase transition of NbO_2 at $T = 1080$ K, undetected in the emf of cells II and III, the derived second-law enthalpies and entropies of NbO_2 and $NbO_{2.422}$ may be slightly distorted. Because of the nonavailability of reliable heat capacity data for oxides of niobium other than NbO_2, accurate values of enthalpy of formation at $T = 298.15$ K can only be derived for NbO_2.

Discussion

NbO: Comparison of the Standard Gibbs Energy of Formation. The Gibbs energy of formation of NbO obtained in this study and those reported in the literature are compared in Figure 2 as a function of temperature. To display clearly the difference between the various studies, the difference between the values obtained by other investigators and those measured in this study is plotted in Figure 2. There are two distinct sets of data for the Gibbs energy of formation of NbO. The values reported by Worrell[20] using ($NbO + NbO_2$), Hiraoka et al.[21] using ($Cr + Cr_2O_3$), and Lavrentév et al.[24] using (Fe + "FeO") as a reference electrode are more negative than the values obtained in this study. However, the values given by Ignatowicz and Davies,[22] Drobyshev and Rezukhina,[23] and Steele and Alcock[25] using (Fe + "FeO") as the reference electrode are more positive.

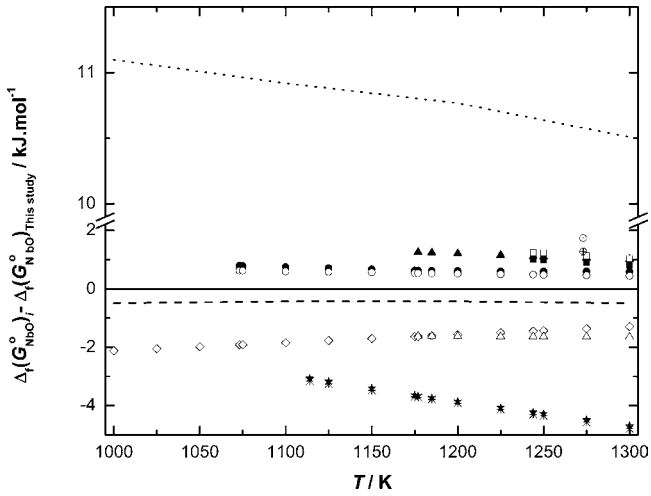

Figure 2. Difference between standard Gibbs energies of formation of NbO reported in the literature $\Delta_f G^o(NbO)_i$ and that obtained in this study $\Delta_f G^o(NbO)_{ThisStudy}$, as a function of temperature T. Measurements: ◇, Worrell;[20] △, Hiraoka et al.;[21] ▲, Hiraoka et al.[21] (corrected); ○, Ignatowicz and Davies;[22] ●, Ignatowicz and Davies[22] (corrected); □, Drobyshev and Rezukhina;[23] ■, Drobyshev and Rezukhina[23] (corrected); ∗, Lavrentév et al.;[24] ★, Lavrentév et al.[24] (corrected); ⊕, Steele and Alcock[25] (Ni + NiO); ⊙, Steele and Alcock[25] (Fe + "FeO"). Compilations: - - -, NIST-JANAF tables;[32] ····, Pankratz and Mrazek.[33]

Table 1. Reassessed Standard Molar Thermodynamic Properties of NbO as a Function of Temperature (T): Heat Capacity at Constant Pressure (C_p^o), Entropy (S^o), Enthalpy Increment ($H_T^o - H_{298.15}^o$), Enthalpy of Formation (ΔH_f^o), and Gibbs Energy of Formation (ΔG_f^o)

	C_p^o	S^o	$H_T^o - H_{298.15}^o$	ΔH_f^o	ΔG_f^o
T/K	(J·mol^{-1}·K^{-1})		(kJ·mol^{-1})		
298.15	41.112	46.024	0	−419.222	−391.490
300	41.187	46.279	0.076	−419.219	−391.319
400	44.032	58.555	4.350	−418.938	−382.055
500	45.827	68.584	8.848	−418.534	−372.879
600	47.204	77.064	13.501	−418.074	−363.792
700	48.369	84.429	18.280	−417.579	−354.784
800	49.467	90.960	23.173	−417.051	−345.847
900	50.481	96.845	28.170	−416.496	−336.980
1000	51.467	102.215	33.268	−415.909	−328.177
1100	52.418	107.165	38.462	−415.289	−319.433
1200	53.359	111.766	43.751	−414.636	−310.748
1300	54.287	116.074	49.134	−413.942	−302.117
1400	55.208	120.131	54.608	−413.213	−293.543
1500	56.117	123.971	60.175	−412.449	−285.022
1600	57.024	127.622	65.132	−412.358	−277.252
1700	57.929	131.106	71.579	−410.848	−268.135
1800	58.831	134.443	77.417	−410.023	−259.762
1900	59.730	137.647	83.345	−409.192	−251.436
2000	60.626	140.734	89.363	−408.358	−243.156
2100	61.526	143.714	95.471	−407.528	−234.917
2200	62.413	146.596	101.668	−406.707	−226.714

Slightly different values for the oxygen chemical potential of the (Fe + "FeO") reference electrode were used in three previous studies.[22−24] For establishing a uniform base for comparisons, the Gibbs energy of formation of NbO was recalculated from the emf values reported in these studies using the oxygen chemical potential of the (Fe + "FeO") reference electrode evaluated recently.[48] In the same way, corrections were also applied to values reported by Hiraoka et al.[21] employing more recent data on the oxygen potential of the (Cr + Cr_2O_3) reference electrode.[49] The corrected values are also presented in Figure 2. The corrected Gibbs energy of formation values of Hiraoka et al.[21] are more positive than the values obtained in this study.

Among the four sets of emf measurements using (Fe + "FeO") as the reference electrode,[22−25] three (Ignatowicz and Davies,[22] Drobyshev and Rezukhina,[23] and Steele and Alcock[25]) are in reasonable agreement. Among these, the higher emf reported by Ignatowicz and Davies[22] is preferred since systematic errors in measurement caused by the presence of trace electronic conduction in the solid electrolyte and polarization of the electrodes and oxygen transfer between electrodes via the gas phase generally yield a lower emf. A significantly larger emf recorded by Lavrentév et al.[24] is probably caused by a temperature gradient across their cell.

The Gibbs energy of formation of NbO reported by Ignatowicz and Davies[22] using (Fe + "FeO") as the reference electrode is in good agreement with the data obtained in this study using (Mn + MnO) as the reference electrode. Since the oxygen potential associated with the (Fe + "FeO") electrode is much higher than that of (Mn + MnO), electrode polarization caused by trace electronic conductivity of the solid electrolyte does not appear to be very significant.

The more negative (∼1.69 kJ·mol^{-1}) values for the Gibbs energy of formation of NbO reported by Worrell[20] arises primarily from the Gibbs energy of formation of NbO_2 taken from the literature,[31] which was used in the calculation. The cell used by Worrell[20] for the measurement of NbO is identical to cell II of this study. The comparison of the emf of the identical cells from the two studies in Figure 1 shows good agreement at T = 1193 K. But the slopes differ; the maximum deviation in emf is ± 4.45 mV, corresponding to a Gibbs energy difference of ± 0.86 kJ·mol^{-1} for NbO.

Values for the Gibbs energy of formation of NbO given in the NIST-JANAF tables[32] are marginally more negative, and values assessed by Pankratz and Mrazek[33] are significantly more positive than those obtained in this study. Low-temperature heat capacity values of NbO are not available in the literature. The values of standard entropy given in NIST-JANAF tables[32] ($S^o_{298.15}$ = 46.024 J·mol^{-1}·K^{-1}) and Pankratz and Mrazek[33] ($S^o_{298.15}$ = 48.116 J·mol^{-1}·K^{-1}) are estimated. The temperature dependence of the Gibbs energy of formation of NbO obtained in this study is very close to that given in the NIST-JANAF tables.[32] Thus, the entropy estimated in the NIST-JANAF tables[32] is supported by the results of this study. A small revision in the enthalpy of formation is suggested. The revised value of $\Delta_f H^o_{298.15}$ is −419.222 (± 3.6) kJ·mol^{-1}. Using the revised value $\Delta_f H^o_{298.15}$, the thermodynamic properties of NbO are re-evaluated in the temperature range T = (298.15 to 2200) K and are presented in Table 1. Low-temperature heat capacity measurements are required to further refine thermodynamic data for NbO.

NbO_2: Comparison of Standard Gibbs Energy of Formation. The Gibbs energy of formation of NbO_2 obtained in this study and those reported in the literature are compared in Figure 3 as a function of temperature. Hiraoka et al.[21] and Marucco et al.[26] measured the emf of solid state electrochemical cells with (NbO + NbO_2) as the working electrode, doped ThO_2 as the electrolyte, and (Cr + Cr_2O_3) as the reference electrode at T = (1117 to 1361) K and T = (1173, 1273, and 1323) K, respectively. The Gibbs energy of formation of NbO_2 was calculated from the emf data by Hiraoka et al.[21] by using their own data for NbO. Since Marucco et al.[26] did not report measurement on NbO, the Gibbs energy of formation of NbO_2 has been calculated from their emf values using data on NbO from this study. Hiraoka et al.[21] and Marucco et al.[26] used different values of the oxygen chemical potential for the (Cr + Cr_2O_3) reference electrode. To establish a uniform base for comparison, the Gibbs energy

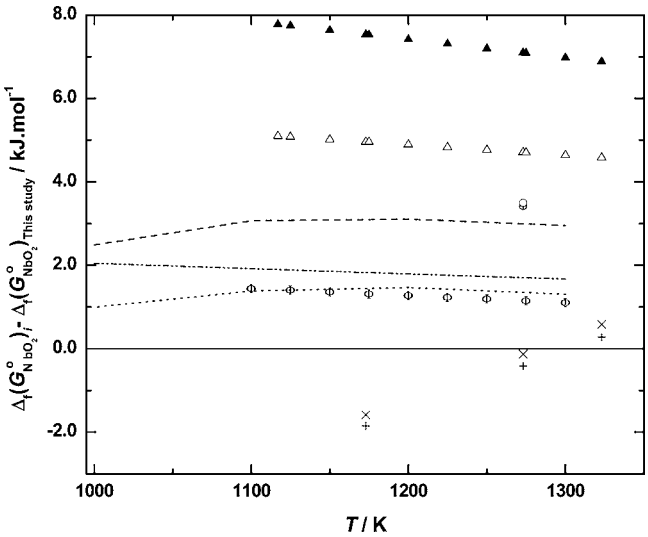

Figure 3. Difference between standard Gibbs energy of formation of NbO_2 reported in the literature $\Delta_f G^o(NbO_2)_i$ and that obtained in this study $\Delta_f G^o(NbO_2)_{ThisStudy}$, as a function of temperature T. Measurements: △, Hiraoka et al.;[21] ▲, Hiraoka et al.[21] (corrected); ⊕, Steele and Alcock;[25] ⊙, Steele and Alcock[25] (corrected); ×, derived from Marucco et al.;[26] +, Marucco et al.[26] (corrected); Φ, Worrell;[27] Compilations: −••−••−, Schick;[31] - - -, NIST- JANAF tables;[32] ••••, Pankratz and Mrazek.[33]

of formation of NbO_2 has been recalculated from their emf using more recent and accurate information on the oxygen chemical potential of the ($Cr + Cr_2O_3$) reference electrode.[49] The corrected values of the Gibbs energy of formation of NbO_2 from the two sources[21,26] are also presented in Figure 3. Worrell[27] determined the Gibbs energy of formation of NbO_2 by measuring the carbon monoxide equilibrium pressure during carbon reduction of Nb_2O_5 to form NbO_2. More recent phase equilibrium data[15−19] shows that there are intermediate phases between Nb_2O_5 and NbO_2. Steele and Alcock[25] measured emf values employing ($NbO + NbO_2$) as the working electrode, doped thoria as the electrolyte, and (Fe + "FeO") as the reference electrode at $T = 1273$ K. Correction using more recent information on the reference electrode[48] does not cause a significant change.

The Gibbs energy of formation of NbO_2 reported in most of the earlier studies is more positive than values obtained in this study. The Gibbs energy of formation of NbO_2 of Worrell[27] is marginally (1.29 kJ·mol^{-1}) more positive, and those reported by Steele and Alcock,[25] Hiraoka et al.,[21] and the corrected values of Hiraoka et al.[21] are progressively more positive than the values obtained in this study. The particle size of NbO_2 powder used in the previous studies is not reported; use of NbO_2 powder in the nanometer size range can result in more positive values. Data derived from the more recent emf measurement of Marucco et al.[26] for the Gibbs energy of formation of NbO_2 agree with the results of this study at $T \approx 1300$ K; their values are more negative at lower temperatures and more positive at higher temperatures, with a maximum deviation of 1.85 kJ·mol^{-1}. The data compiled by Schick[31] Pankratz and Mrazek[33] and the NIST-JANAF tables[32] are also more positive than the values obtained in this study. The change in the slope of the Gibbs energy of formation of NbO_2 given in the NIST-JANAF tables[32] and by Pankratz and Mrazek[33] is caused by the phase transition at $T =$ 1080 K from a low-temperature distorted rutile to a high-temperature rutile structure.

The standard enthalpy of formation of NbO_2 at $T = 298.15$ K can be derived from the Gibbs energy of formation obtained in this study by a third-law analysis using the equation:

$$\Delta_f H^o_{298.15} = \Delta_f G^o_T - \Delta(H^o_T - H^o_{298.15}) + T\{\Delta_f S^o_{298.15} + \Delta(S^o_T - S^o_{298.15})\} \quad (10)$$

where $(H^o_T - H^o_{298.15})$ and $(S^o_T - S^o_{298.15})$ for each phase can be calculated using the integrals: $\int_{298.15}^{T} C^o_p\, dT$ and $\int_{298.15}^{T} (C^o_p/T)\, dT$, respectively. The quantities $\Delta(H^o_T - H^o_{298.15})$ and $\Delta(S^o_T - S^o_{298.15})$ represent the difference of $\sum\delta_i(H^o_T - H^o_{298.15})$ and $\sum\delta_i(S^o_T - S^o_{298.15})$ between the products and the reactants, respectively, and δ_i is the stoichiometric coefficient for element or compound i. To assess the best value of the standard entropy of NbO_2 at $T = 298.15$ K used in eq 10, a re-examination of the low-temperature heat capacity data of NbO_2 is warranted in view of the new measurements reported in the literature.

NbO_2: Low-Temperature Heat Capacity and Entropy at $T = 298.15$ K. The heat capacity of the low-temperature modification of NbO_2 has been measured recently by Wenger and Keesom[28] in the temperature range $T =$ (2.5 to 26.3) K. King[29] measured the heat capacity in the temperature range $T =$ (53.45 to 298.15) K. The variation of the heat capacity of NbO_2 in the temperature range $T =$ (0 to 298.15) K is shown in Figure 4. From the combined data, the standard entropy ($S^o_{298.15}$) at $T =$ 298.15 K is calculated as ($S^o_{298.15} \pm 0.27 = 54.249$/J·K^{-1}·mol^{-1}), in good agreement with the value used in the NIST-JANAF tables[32] ($S^o_{298.15} \pm 0.29 = 54.506$/J·K^{-1}·mol^{-1}). Thus, the new measurements do not significantly affect the values of the standard entropy at $T = 298.15$ K.

NbO_2: High-Temperature Heat Capacity. King and Christensen[30] measured the heat content ($H_T - H_{298.15}$) of NbO_2 over the temperature range $T =$ (399.3 to 1790.8) K and reported two anomalies at $T =$ (1090 and 1200) K. The data compiled in the NIST-JANAF tables[32] are based on the measurements of King and Christensen.[30] Subsequent studies[34,50,51] on NbO_2 have found only one higher order phase transition with a peak at $T \sim 1080$ K. Seta and Naito[34] simultaneously measured the heat capacity and electrical conductivity of NbO_2 in the temperature range $T =$ (400 to 1170) K using direct heating pulse calorimetry and reported a phase transition at $T = 1080$ K. Janninck and Whitmore[50] measured the electrical conductivity and thermoelectric power of NbO_2 in the temperature range $T =$ (196 to 1273) K and found irregular behavior in electrical conductivity and thermoelectric power measurements at $T = 1070$ K

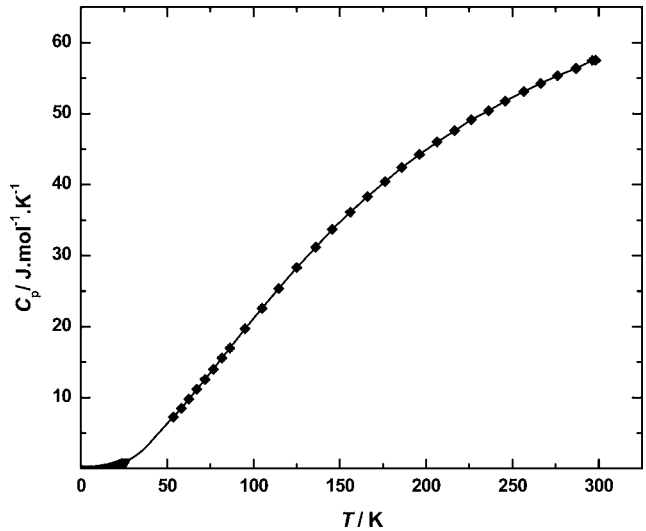

Figure 4. Low-temperature heat capacity NbO_2 in the temperature range $T =$ (0 to 298.15) K. ▼, Wenger and Keesom;[28] ♦, King;[29] —, data assessed in this study.

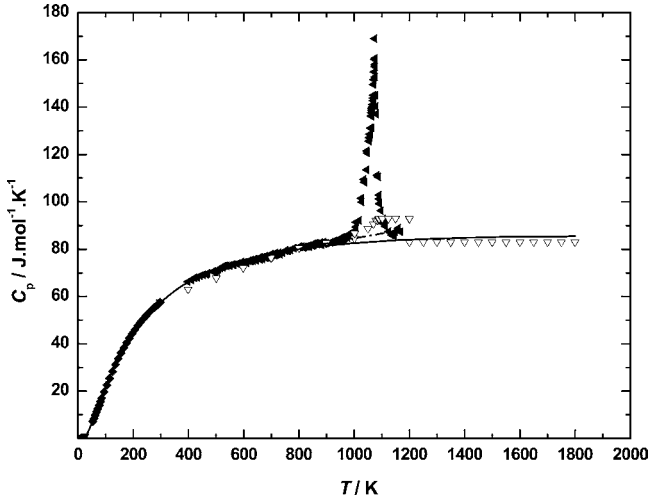

Figure 5. Heat capacity of NbO_2 in the temperature range $T = (0$ to $1800)$ K. ▼, Wenger and Keesom;[28] ♦, King;[29] ▽, King and Christensen;[30] solid left-pointing triangle, Sita and Naito;[34] −•−•−, heat capacity equation proposed by Sita and Naito[34] in the temperature range $T = (400$ to $1150)$ K excluding the anomalous region; —, data assessed in this study in the temperature range $T = (298.15$ to $1800)$ K is represented by eq 11, excluding the anomalous region.

indicating a phase change or an insulator to metal transition. On the basis of recent studies,[34,50] the phase transition temperature of NbO_2 in this study is taken as $T = 1080$ K. Plotted in Figure 5 is the variation of the heat capacity of NbO_2 in the temperature range $T = (0$ to $1800)$ K. The heat capacities derived from the high temperature heat content measurement of King and Christensen[30] are compared with the direct measurements of Seta and Naito.[34] Except in the vicinity of the transition, the combined data can be represented by the empirical equation in the temperature range $T = (298.15$ to $1800)$ K:

$$C_p^o/\mathrm{J\cdot mol^{-1}\cdot K^{-1}} = 135.82 - 0.01468(T/\mathrm{K}) - 1282.3(T/\mathrm{K})^{-1/2} + 1.9477\cdot 10^{-6}(T/\mathrm{K})^2 \quad (11)$$

At $T > 1080$ K, the equation suggests a small increase in heat capacity with temperature, in contrast to the constant value suggested by King and Christensen.[30] The difference between the experimental C_p values of Sita and Naito[34] and that given by eq 11 in the temperature range $T = (760.8$ to $1158)$ K was taken as the contribution from the phase transition. Integrating $C_{p(tr)}/T$ versus T, the phase transition entropy ($\Delta S_{tr} = 3.165$ J·mol^{-1}·K^{-1}) is obtained. For the purpose of compiling a thermodynamic data table, the higher order phase transition in NbO_2 may be treated as an equivalent first-order transition. Heat content ($H_T - H_{298.15}$) values derived from the heat capacity data of Sita and Naito[34] compare well with the values reported by King and Christensen[30] as shown in Figure 6. The data assessed in this study reproduce the experimental data well except in the immediate vicinity of the phase transition.

NbO_2: Enthalpy of Formation at $T = 298.15$ K. The standard enthalpy of formation of NbO_2 is obtained from the Gibbs energy of formation of NbO_2 obtained in this study by applying eq 10. Since the effect of the phase transition of NbO_2 on heat capacity extends from $T = (760.8$ to $1158)$ K,[34] the Gibbs energy of formation of NbO_2 in the temperature range $T = (1200$ to $1300)$ K is used to calculate the standard enthalpy of formation of NbO_2 ($\Delta_f H^o_{298.15} = -796.785 \pm 0.25$ kJ·mol^{-1}) using the third-law method. The reassessed value of $\Delta_f H^o_{298.15}$ is 1.915 kJ·mol^{-1}, more negative than the value given in the NIST-JANAF tables.[32]

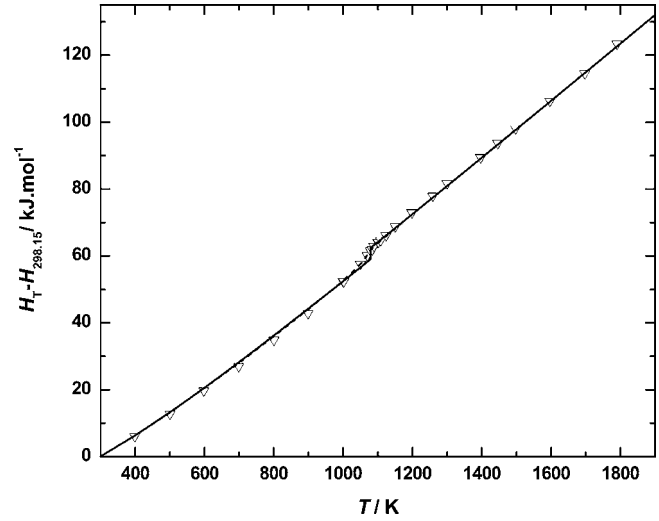

Figure 6. Variation of heat content of NbO_2 as a function of temperature in the temperature range $T = (400$ to $1800)$ K. ▽, King and Christensen;[30] ---, calculated from C_p data of Seta and Naito;[34] —, data assessed in this study.

Table 2. Reassessed Standard Molar Thermodynamic Properties of NbO_2 as a Function of Temperature (T): Heat Capacity at Constant Pressure (C_p^o), Entropy (S^o), Enthalpy Increment ($H_T^o - H_{298.15}^o$), Enthalpy of Formation (ΔH_f^o), and Gibbs Energy of Formation (ΔG_f^o)

	C_p^o	S^o	$H_T^o - H_{298.15}^o$	ΔH_f^o	ΔG_f^o
T/K	(J·mol^{-1}·K^{-1})		(kJ·mol^{-1})		
298.15	57.353	54.249	0	−796.785	−740.923
300	57.557	54.605	0.106	−796.779	−740.577
400	66.144	72.440	6.327	−796.036	−721.934
500	71.620	87.830	13.233	−794.754	−703.548
600	75.363	101.239	20.594	−793.166	−685.454
700	78.032	113.068	28.271	−791.400	−667.639
800	79.986	123.621	36.177	−789.528	−650.085
900	81.442	133.131	44.251	−787.598	−632.770
1000	82.537	141.771	52.453	−785.638	−615.673
1080	83.218	148.150	59.084	−784.070	−601.534
1080	83.218	151.315	62.502	−780.652	−601.534
1100	83.366	152.843	64.168	−780.252	−598.834
1200	83.992	160.125	72.538	−778.309	−582.447
1300	84.463	166.868	80.962	−776.349	−566.186
1400	84.814	173.140	89.426	−774.436	−550.091
1500	85.073	179.001	97.921	−772.565	−534.133
1600	85.260	184.498	106.439	−770.747	−518.297
1700	85.392	189.671	114.972	−768.997	−502.574
1800	85.482	194.555	123.516	−767.323	−486.948

Using the high-temperature heat capacity of NbO_2 from eq 11, the standard enthalpy of formation ($\Delta_f H^o_{298.15} = -796.785$ kJ·mol^{-1}), standard entropy ($S^o_{298.15} = 54.249$ J·mol^{-1}·K^{-1}), phase transition at $T = 1080$ K, enthalpy of transition ($\Delta H_{tr} = 3.418$ kJ·mol^{-1}), and entropy of transition ($\Delta S_{tr} = 3.165$ J·mol^{-1}·K^{-1}), the thermodynamic properties of NbO_2 have been reassessed in the temperature range $T = (298.15$ to $1800)$ K and are presented in Table 2. The thermodynamic properties reassessed in this study differ significantly from the values present in thermodynamic compilations[31−33] as shown in the Figure 3.

$NbO_{2.422}$: Comparison of the Standard Gibbs Energy of Formation. The Gibbs energy of formation of $NbO_{2.422}$ obtained in this study and those reported in the literature are compared in Figure 7 as a function of temperature. Worrell[20] measured emf values using two different solid state electrochemical cells with ($NbO_2 + Nb_2O_{4.8}$) as the working electrode, doped ThO_2

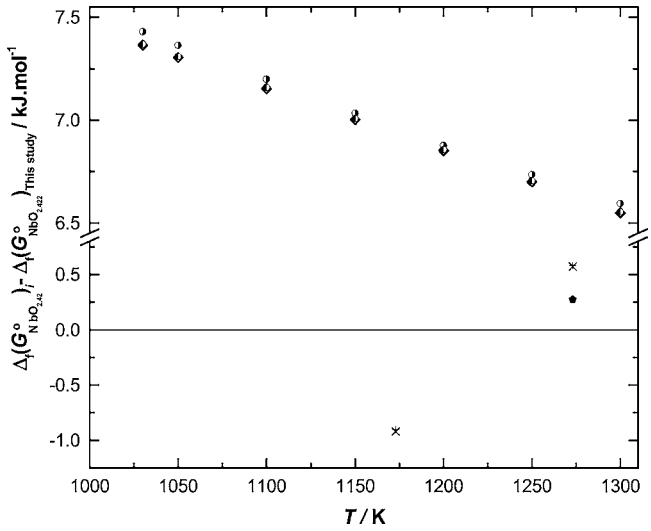

Figure 7. Difference between the standard Gibbs energy of formation of $NbO_{2.42}$ ($Nb_{12}O_{29}$) reported in the literature $\Delta_f G^o(NbO_{2.42})_i$ and that obtained in this study $\Delta_f G^o(NbO_{2.422})_{ThisStudy}$, as a function of temperature T. ◇, Worrell[20] (cell "A"); ◐, Worrell[20] (cell "B"); ◑, Worrell[20] (corrected cell "B"); solid pentagon, Marucco;[16] ×, Marucco et al.;[26] +, Marucco et al.[26] (corrected).

as the electrolyte, and (NbO + NbO_2) and (Fe + "FeO") as reference electrodes at T = (1030 to 1300) K. It is assumed that the phase identified by Worrell[20] as $Nb_2O_{4.8}$ is the same as the $NbO_{2.422}$ found in this study. The solid state electrochemical cell used by Worrell[20] with the (NbO + NbO_2) reference will hereafter be designated as cell "A" and the cell with the (Fe + "FeO") reference electrode as cell "B". Cell "A" of Worrell[20] is identical to cell III of this study. The comparison of the emf's in Figure 1 shows that the values reported by Worrell[20] are significantly lower than that obtained in this study. Worrell[20] calculated the free energy of formation of $Nb_2O_{4.8}$ from the emf of cell "A" using the free energy of formation of NbO from his own measurements and that of NbO_2 from Schick.[31] From the emf of cell "B", Worrell[20] calculated the Gibbs energy of formation of $Nb_2O_{4.8}$ ($NbO_{2.4}$) using the Gibbs energy of formation of NbO_2 by Schick[31] and a value of the oxygen chemical potential of the reference electrode (Fe + "FeO") from Blumenthal and Whitmore.[52] Marucco et al.[26] measured emf using a solid state electrochemical cell similar to cell "B" in the temperature range T = (1173 to 1323) K. The Gibbs energy of formation of $NbO_{2.42}$ was calculated from emf using data for NbO_2 derived from their own measurements on the phase mixture (NbO + NbO_2)[26] in conjunction with the Gibbs energy of formation of NbO obtained in this study. Since Worrell[20] and Marucco et al.[26] used different values for the oxygen chemical potential of the (Fe + "FeO") reference electrode, their values of free energy of formation of $NbO_{2.422}$ were recalculated using more recent information on the oxygen potential of the (Fe + "FeO") reference.[48] Corrected values are also shown in Figure 7. Marucco[16] measured the oxygen partial pressure in equilibrium with niobium oxides in the temperature range T = (1273 to 1373) K using a CO/CO_2 gas equilibrium technique and thermogravimetry to detect the change in composition. The Gibbs energy of formation of $NbO_{2.42}$ from the data of Marucco[16] was obtained using the Gibbs energy of formation of NbO_2 from Marucco et al.[26] and that of NbO from this study.

The Gibbs energy of formation of $NbO_{2.4}$ reported by Worrell[20] are more positive by (6.55 to 7.43) kJ·mol^{-1} than the values obtained in this study in the temperature range T = (1030 to 1300) K. The data of Marucco et al.[26] agrees with the value obtained in this study at $T \approx 1234$ K. Their values are more negative at lower temperatures and more positive at higher temperatures with maximum deviations less than 0.92 kJ·mol^{-1}.

Gibbs Energy of Mixing for the System Nb−O at T = 1223 K. It is instructive to compare the relative stabilities of the different oxides of niobium on a plot of the Gibbs energy of mixing as a function of composition at constant temperature. For illustration T = 1223 K is selected. For constructing the Gibbs energy of mixing plot, values for nonstoichiometric Nb_2O_{5-x} have to be evaluated. Several groups[16−19,45,47] have investigated thermodynamic properties of nonstoichiometric Nb_2O_{5-x}. In a review of data on nonstoichiometric Nb_2O_{5-x}, Naito and Matsui[18] found several inconsistencies. These were partially resolved by new measurements[19] of the partial molar free energy of oxygen in Nb_2O_{5-x} ($2.47 \le$ O/Nb ≤ 2.50) for different compositions as a function of temperature using a galvanic cell in the range T = (1084 to 1325) K. The data of Matsui and Naito[19] show that ln x in Nb_2O_{5-x} versus ln $P_{O_2}/2$ has a slope of −5.2, for an O/Nb ratio = (2.50 to 2.49), and a slope of −3 for O/Nb ratio = (2.490 to 2.477). Using this data, the activity of niobium at temperature T = 1223 K for different compositions of Nb_2O_{5-x} is calculated using the Gibbs−Duhem equation:

$$[\ln a_{Nb}]_{X_{Nb}} = -\int_{X_{Nb}=0.28571}^{X_{Nb}} \frac{1}{2}\frac{X_o}{X_{Nb}} d\ln P_{o_2} + [\ln a_{Nb}]_{X_{Nb}=0.28571} \quad (12)$$

where the first term on the right-hand side of the eq 12 defines the change of activity of niobium with composition in the nonstoichiometric range and the second term represents the activity of niobium in stoichiometric Nb_2O_5. Assuming that the oxide is stoichiometric at the standard pressure ($1.01 \cdot 10^5$ Pa) of diatomic oxygen gas, the activity of Nb can be derived from the standard free energy of formation of Nb_2O_5. First, NIST-JANAF[32] data for Nb_2O_5 were used to obtain the activity of Nb in Nb_2O_5 in equilibrium with pure oxygen. Then the activity of Nb was evaluated as a function of composition. The Gibbs energy of mixing for nonstoichiometric compositions of Nb_2O_{5-x} was computed by combining the activities of both components:

$$\Delta G_m = RT(X_{Nb} \ln a_{Nb} + X_O \ln P_{O_2}/2) \quad (13)$$

Presented in Table 3 is the Gibbs energy of mixing at different compositions corresponding to the compounds NbO, NbO_2, $NbO_{2.422}$, and oxygen-deficient Nb_2O_{5-x} compositions. Values of the Gibbs energy of mixing of NbO, NbO_2, and $NbO_{2.422}$ at T = 1223 K is calculated from eqs 5, 7, and 9, respectively. The results are displayed in Figure 8a, and an expanded view is presented in Figure 8b. It is seen that the Gibbs energy of mixing curve for Nb_2O_{5-x} based on the NIST-JANAF[32] data does not generate the correct phase boundary of nonstoichiometric Nb_2O_{5-x} ($X_o = 0.7124$) given by Naito et al.[17] (O/Nb = 2.477 at T = 1233 K).

To obtain a match between thermodynamic data on the suboxides obtained in this study and the phase diagram, the Gibbs energy of formation of Nb_2O_5 has to be increased by 1.23 kJ·mol^{-1}. The corresponding activity of niobium in stoichiometric Nb_2O_5 thus obtained is $6.097 \cdot 10^{-30}$. The activity of Nb and Gibbs energy of mixing for the Nb_2O_{5-x} phase were recalculated, and the latter is plotted in Figure 8a,b. The tangent construction now gives the correct phase boundary. It is seen

Table 3. Variation in the Gibbs Energy of Mixing (ΔG^M) of the Different Phases (O/Nb Ratio) Present in the Nb−O System at Temperature $T = 1223$ K

O/Nb ratio	ΔG^M (+)[a]	ΔG^M (++)[b]
	kJ·mol^{-1}	
1.0000	−154.377	−154.377
2.0000	−192.919	−192.919
2.4220	−195.494	−195.494
2.4771	−195.555	−195.732
2.4802	−195.558	−195.735
2.4900	−195.549	−195.725
2.4945	−195.526	−195.703
2.4977	−195.493	−195.669
2.4982	−195.486	−195.662
2.4990	−195.471	−195.647
2.4994	−195.462	−195.638
2.5000	−195.438	−195.614

[a] (+), based on reassessed data for Nb_2O_5 ($\Delta G_f^o = -1368.07$ kJ·mol^{-1}). [b] (++), based on NIST-JANAF tables[32] for Nb_2O_5 ($\Delta G_f^o = -1369.30$ kJ·mol^{-1}).

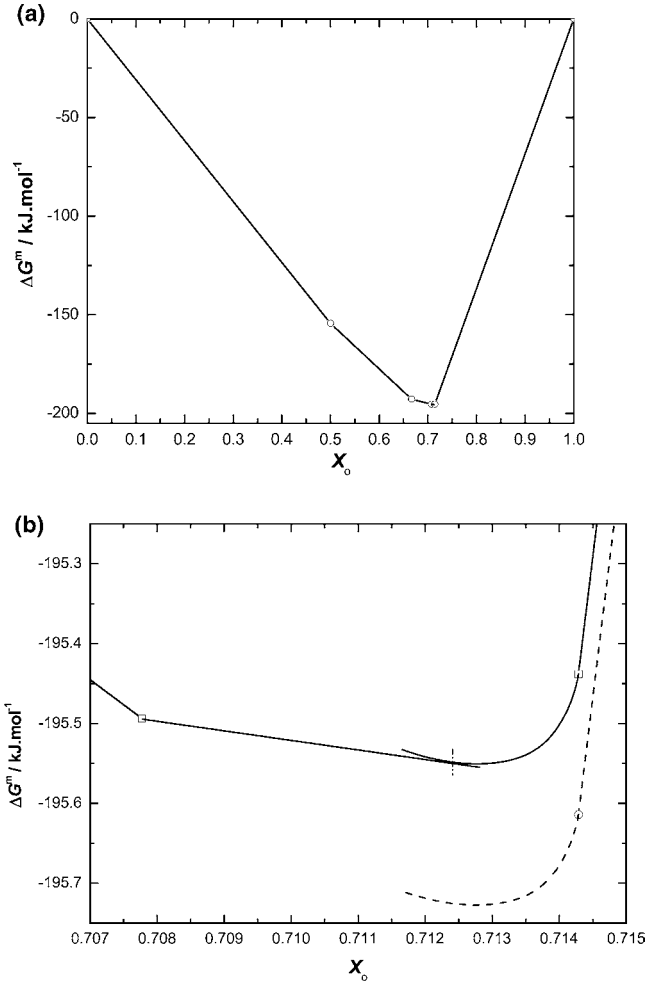

Figure 8. (a) Gibbs energy of mixing for the system Nb−O at $T = 1223$ K. (b) Expanded view of the Gibbs energy of mixing at $T = 1223$ K near the minimum. —, reassessed data; - - -, based on NIST-JANAF tables.[32] The straight line ($0.7078 \le X_o \le 0.7124$) is the common tangent that defines the phase boundary of Nb_2O_{5-x} in equilibrium with $NbO_{2.422}$.

that oxides containing Nb in the lower valency states are relatively less stable than oxides containing Nb in higher valency state. The minimum of the Gibbs energy of mixing occurs at $X_o = 0.7128$ corresponding to O/Nb = 2.482 in nonstoichiometric Nb_2O_{5-x} ($x = 0.036$). The oxygen-deficient Nb_2O_{5-x} compositions are more stable than the stoichiometric Nb_2O_5.

Table 4. Reassessed Standard Molar Thermodynamic Properties of α-Nb_2O_5 as a Function of Temperature (T): Heat Capacity at Constant Pressure (C_p^o), Entropy (S^o), Enthalpy Increment ($H_T^o - H_{298.15}^o$), Enthalpy of Formation (ΔH_f^o), and Gibbs Energy of Formation (ΔG_f^o)

T/K	C_p^o	S^o	$H_T^o - H_{298.15}^o$	ΔH_f^o	ΔG_f^o
	(J·mol^{-1}·K^{-1})		(kJ·mol^{-1})		
298.15	131.988	137.298	0	−1898.305	−1764.585
300	132.320	138.115	0.244	−1898.288	−1763.756
400	144.992	178.096	14.172	−1896.802	−1719.108
500	153.841	211.441	29.131	−1894.620	−1674.926
600	160.737	240.126	44.875	−1892.002	−1631.230
700	166.013	265.318	61.225	−1889.102	−1587.994
800	170.038	287.760	78.035	−1886.026	−1545.185
900	173.117	307.972	95.199	−1882.854	−1502.771
1000	175.502	326.340	112.634	−1879.634	−1460.714
1100	177.360	343.157	130.280	−1876.401	−1418.977
1200	178.328	358.654	148.092	−1873.184	−1377.537
1300	179.991	373.016	166.035	−1869.994	−1336.361
1400	180.920	386.390	184.082	−1866.855	−1295.429
1500	181.665	398.898	202.213	−1863.794	−1254.722
1600	182.263	410.642	220.410	−1860.830	−1214.214
1700	182.745	421.707	238.661	−1857.991	−1173.892

On the basis of the change in Gibbs energy of formation of Nb_2O_5 at $T = 1223$ K, a small revision in the enthalpy of formation of stoichiometric Nb_2O_5 is suggested. The revised value of $\Delta_f H_{298.15}^o$ is −1898.305 (± 2.1) kJ·mol^{-1}, more positive by 1.23 kJ·mol^{-1} than the value in NIST-JANAF.[32] The reassessed value of the standard enthalpy of formation is closer to the value given by Pankratz and Mrazek,[33] only 0.246 kJ·mol^{-1} more positive. Using the revised value of $\Delta_f H_{298.15}^o$ and other thermodynamic functions from NIST-JANAF,[32] the thermodynamic properties of Nb_2O_5 are re-evaluated in the temperature range $T = (298.15$ to 1700) K and are presented in Table 4.

Conclusions

The Gibbs energy of formation of NbO, NbO_2, and $NbO_{2.422}$ has been measured using high-temperature electrochemical measurements in the temperature range $T = (1000$ to 1300) K. The data obtained for NbO are in reasonable accord with values given in the NIST-JANAF tables.[32] The Gibbs energy of formation of NbO_2 obtained in this study is significantly more negative (~3 kJ·mol^{-1}) than those in NIST-JANAF tables.[32] On the basis of new measurements and a critical assessment of calorimetric data in the literature, a revised thermodynamic data table for NbO and NbO_2 is presented. For $NbO_{2.422}$ ($Nb_{12}O_{29}$), the new measurements refine limited Gibbs energy data available in the literature. The Gibbs energy of formation of stoichiometric Nb_2O_5 in the NIST-JANAF tables[32] has to be revised upward by 1.23 kJ·mol^{-1} to obtain the consistency between the data for $NbO_{2.422}$ obtained in this study and phase boundary compositions. The minimum in the Gibbs energy of mixing for the system Nb−O at $T = 1223$ K occurs at a O/Nb ratio of 2.482 corresponding to Nb_2O_{5-x} ($x = 0.036$). The nonstoichiometric Nb_2O_{5-x} is more stable than stoichiometric Nb_2O_5 and other oxide phases. The presence of defects increases the stability of Nb_2O_5.

Literature Cited

(1) Smith, D. L.; Majumdar, S.; Billone, M.; Mattas, R. Performance limits for fusion first-wall structural materials. *J. Nucl. Mater.* **2000**, *283*−*287*, 716–720.
(2) Gao, W.; Conley, J. F. J.; Ono, Y. NbO as gate electrode for n-channel metal-oxide-semiconductor field-effect-transistors. *Appl. Phys. Lett.* **2004**, *84*, 4666–4668.

(3) Shin, S. H.; Halpern, T.; Raccah, P. M. High-speed high-current field switching of NbO_2. *J. Appl. Phys.* **1977**, *48*, 3150–3153.
(4) Vezzoli, G. C.; Levy, S.; Lalevic, B.; Shoga, M. Threshold switching polycrystalline NbO_2: decay and recovery of the on state at room and low temperatures and its relationship to the trapping centers. *J. Appl. Phys.* **1983**, *54*, 5828–5838.
(5) Vezzoli, G. C.; Doremus, L. W.; Levy, S.; Gaule, G. K.; Lalevic, B.; Shoga, M. The on-state of single-crystal and polycrystalline NbO_2. *J. Appl. Phys.* **1981**, *52*, 833–839.
(6) Thomas, C. B.; Lettington, A. H. The characteristics of monostable switching in amorphous niobate films. *J. Phys. D: Appl. Phys.* **1977**, *10*, 1965–1973.
(7) Emmenegger, F. P.; Robinson, M. L. A. Preparation and dielectric properties of niobium pentoxide crystals. *J. Phys. Chem. Solids* **1968**, *29*, 1673–1681.
(8) Reichman, B.; Bard, A. J. Electrochromism at niobium pentoxide electrodes in aqueous and acetonitrile solutions. *J. Electrochem. Soc.* **1980**, *127*, 241–242.
(9) Dyer, C. K.; Leach, J. S. L. Reversible optical changes within anodic oxide films on titanium and niobium. *J. Electrochem. Soc.* **1978**, *125*, 23–29.
(10) Yoshimura, K.; Miki, T.; Iwama, S.; Tanemura, S. Characterization of niobium oxide electrochromic thin films prepared by reactive d. c. magnetron sputtering. *Thin Solid Films* **1996**, *281*−*282*, 235–238.
(11) Iizuka, T.; Ogasawara, K.; Tanabe, K. Acidic and catalytic properties of niobium pentaoxide. *Bull. Chem. Soc. Jpn.* **1983**, *56*, 2927–2931.
(12) Murakami, Y.; Wada, Y.; Morikawa, A. Catalytic activity of non-stoichiometric niobium oxide with controlled composition, $NbO_{2.488-2.500}$, for butene isomerization. *Bull. Chem. Soc. Jpn.* **1988**, *61*, 2747–2752.
(13) Brunner, H. R.; Emmenegger, F. P.; Robinson, M. L. A.; Rotschi, H. Growth and properties of Nb_2O_5 thin film capacitors. *J. Electrochem. Soc.* **1968**, *115*, 1287–1289.
(14) Massalski, T. B.; Okamoto, H.; Subramanian, P. R.; Kacprzak, L. *Binary alloy phase diagram*, 2nd ed.; ASM International: Materials Park, OH, 1990; Vol. 2.
(15) Kimura, S. Phase equilibria in the system NbO_2-Nb_2O_5: phase relations at 1300 and 1400 °C and related thermodynamic treatment. *J. Solid State Chem.* **1973**, *6*, 438–449.
(16) Marucco, J. F. Thermodynamic study of the system NbO_2-Nb_2O_5 at high temperature. *J. Solid State Chem.* **1974**, *10*, 211–218.
(17) Naito, K.; Kamegashira, N.; Sasaki, N. Phase equilibria in the system between NbO_2 and Nb_2O_5 at high temperatures. *J. Solid State Chem.* **1980**, *35*, 305–311.
(18) Naito, K.; Matsui, T. Review on phase equilibria and defect structures in the niobium-oxygen system. *Solid State Ionics* **1984**, *12*, 125–134.
(19) Matsui, T.; Naito, K. Thermodynamic study of niobium oxides with O/Nb ratios from 2.47 to 2.50 using a high-temperature galvanic cell. *J. Solid State Chem.* **1985**, *59*, 228–236.
(20) Worrell, W. L. Measurement of the thermodynamic stabilities of the niobium and tantalum oxides using a high-temperature galvanic cell. *Thermodynamics*; International Atomic Energy Agency: Vienna, 1966; Vol. 1, 131−143.
(21) Hiraoka, T.; Sano, N.; Matsushita, Y. The electrochemical measurement of the standard free energy of formation of niobium oxides. *Trans. Iron Steel Inst. Jpn.* **1969**, *55*, 470–474.
(22) Ignatowicz, S.; Davies, M. W. The free energy of formation of NbO and Ta_2O_5. *J. Less-Common Met.* **1968**, *15*, 100–102.
(23) Drobyshev, V. N.; Rezukhina, T. N. Thermodynamic properties of cobalt-niobium alloys. *Russ. J. Phys. Chem.* **1965**, *39*, 75–78.
(24) Lavrentév, V. L.; Gerasimov, Y. L.; Rezukhina, T. N. Thermodynamic characteristics of niobium oxides; equilibrium with hydrogen and electrochemical measurements. *Dokl. Akad. Nauk SSSR* **1961**, *136*, 1372–1378.
(25) Steele, B. C. H.; Alcock, C. B. Factors influencing the performance of solid oxide electrolytes in high temperature thermodynamic measurements. *Trans. Metall. Soc. AIME* **1965**, *233*, 1359–1367.
(26) Marucco, J. F.; Tetot, R.; Gerdanian, P.; Picard, C. Etude thermodynamique du dioxyde de niobium a haute temperature. *J. Solid State Chem.* **1976**, *18*, 97–110.
(27) Worrell, W. L. The free energy of formation of niobium dioxide between 1100 and 1700 K. *J. Phys. Chem.* **1964**, *68*, 952–953.
(28) Wenger, L. E.; Keesom, P. H. Specific heat of NbO_2 at low temperatures. *Phys. Rev. B* **1977**, *15*, 5953–5956.
(29) King, E. G. Low temperature heat capacities and entropies at 298.15 K of some oxides of gallium, germanium, molybdenum and niobium. *J. Am. Chem. Soc.* **1958**, *80*, 1799–1800.
(30) King, E. G.; Christensen, A. U. High temperature heat content and entropy of cerium dioxide and columbium dioxide. *Bur. Mines Rep. Invest.* **1961**, *5789*, 1–6.
(31) Schick, H. L. *Thermodynamics of certain refractory compounds*; Academic Press: New York, 1966; Vol. II.
(32) Chase, M. W.; Davis, C. A.; Downey, J. R.; Frurip, D. J.; McDonald, R. A.; Syverud, A. N. JANAF thermodynamical tables, third ed. *J. Phys. Chem. Ref. Data* **1985**, *14*, 1608–1618.
(33) Pankratz, L. B.; Mrazek, R. V. *Thermodynamical properties of elements and oxides*; U.S. Bureau of Mines: Washington, DC, 1984.
(34) Seta, K.; Naito, K. Calorimetric study of the phase transition in NbO_2. *J. Chem. Thermodyn.* **1982**, *14*, 921–935.
(35) Bowman, A. L.; Wallace, T. C.; Yarnell, J. L.; Wenzel, R. G. The crystal structure of niobium monoxide. *Acta Crystallogr.* **1966**, *21*, 843.
(36) Bolzan, A. A.; Fong, C.; Kennedy, B. J.; Howard, C. J. A powder neutron diffraction study of semi conducting and metallic niobium dioxide. *J. Solid State Chem.* **1994**, *113*, 9–14.
(37) McQueen, T.; Xu, Q.; Andersen, E. N.; Zandbergen, H. W.; Cava, R. J. Structures of the reduced niobium oxides $Nb_{12}O_{29}$ and $Nb_{22}O_{54}$. *J. Solid State Chem.* **2007**, *180*, 2864–2870.
(38) Norin, R. Crystal structure of $Nb_{12}O_{29}$ (Mon). *Acta Chem. Scand.* **1966**, *20*, 871–880.
(39) Andersen, E. N.; Klimczuk, T.; Miller, V. L.; Zandbergen, H. W.; Cava, R. J. Nanometer structural columns and frustration of magnetic ordering in $Nb_{12}O_{29}$. *Phys. Rev. B* **2005**, *72*, 033413-1−4.
(40) Riesman, A.; Holtzberg, F. *High Temperature Oxides*; Academic Press: New York, 1970; Vol. 5.
(41) Gatehouse, B. M.; Wadsley, A. D. The crystal structure of the high temperature form of niobium pentoxide. *Acta Crystallogr.* **1964**, *17*, 1545–1554.
(42) Okaz, A. M.; Keesom, P. H. Specific heat and magnetization of the superconducting monoxides: NbO and TiO. *Phys. Rev. B* **1975**, *12*, 4917–4928.
(43) Brauer, V. G. Die Oxyde des Niobs. *Z. Anorg. Allg. Chem.* **1941**, *248*, 1–31.
(44) Schafer, V. H.; Bergner, D.; Gruehn, R. Die thermodynamische stabilitat der sieben zwischen 2.00 und 2.50 O/Nb existierenden phasen. *Z. Anorg. Allg. Chem.* **1969**, *365*, 31–50.
(45) Kofstad, P.; Anderson, P. B. Gravimetric studies of the defect structure of α-Nb_2O_5. *J. Phys. Chem. Solids* **1961**, *21*, 280–286.
(46) Marucco, J. F. Electrical resistance and defect structure of stable and metastable phases of the system $Nb_{12}O_{29}$−Nb_2O_5 between 800−1100 °C. *J. Chem. Phys.* **1979**, *70*, 649–654.
(47) Blumenthal, R. N.; Moser, J. B.; Whitmore, D. H. Thermodynamic study of non-stoichiometric niobium pentoxide. *J. Am. Ceram. Soc.* **1965**, *48*, 617–622.
(48) Jacob, K. T.; Kumar, A.; Waseda, Y. Gibbs energy of formation of MnO: measurement and assessment. *J. Phase Equilib. Diffus.* **2008**, *29*, 222–230.
(49) Jacob, K. T. Potentiometric determination of the Gibbs energy formation of cadmium and magnesium chromates. *J. Electrochem. Soc.* **1977**, *124*, 1827–1831.
(50) Janninck, R. F.; Whitmore, D. H. Electrical conductivity and thermoelectric power of Niobium dioxide. *J. Phys. Chem. Solids* **1966**, *27*, 1183–1187.
(51) Shapiro, S. M.; Axe, J. D.; Shirane, G.; Raccah, P. M. Neutron scattering study of the structural phase transition of NbO_2. *Solid State Commun.* **1974**, *15*, 377–381.
(52) Blumenthal, R. N.; Whitmore, D. H. Electrochemical measurements of elevated-temperature thermodynamic properties of certain iron and manganese oxide mixtures. *J. Am. Ceram. Soc.* **1961**, *44*, 508–512.

Received for review May 3, 2010. Accepted August 7, 2010. One of the authors (K.T.J.) is grateful to the Indian National Academy of Engineering for support as a INAE Distinguished Professor at the Indian Institute of Science, Bangalore.

JE1004609